Article

Negative Temperature Coefficient Properties of Natural Clinoptilolite

Loredana Schiavo [1], Lucrezia Aversa [2], Roberto Verucchi [2], Rachele Castaldo [3], Gennaro Gentile [3] and Gianfranco Carotenuto [1,*]

[1] Institute of Polymers, Composites and Biomaterials, National Research Council, Piazzale E. Fermi 1, 80055 Portici, Italy; loredana.schiavo@cnr.it

[2] Institute of Materials for Electronics and Magnetism, National Research Council, Trento Unit c/o Fondazione Bruno Kessler, Via alla Cascata 56/C, 38123 Trento, Italy; lucrezia.aversa@cnr.it (L.A.); roberto.verucchi@cnr.it (R.V.)

[3] Institute of Polymers, Composites and Biomaterials, National Research Council, Via Campi Flegrei 34, 80078 Pozzuoli, Italy; rachele.castaldo@cnr.it (R.C.); gennaro.gentile@cnr.it (G.G.)

* Correspondence: giancaro@unina.it

Abstract: Negative temperature coefficient (NTC) materials are usually based on ceramic semiconductors, and electrons are involved in their transport mechanism. A new type of NTC material, adequate for alternating current (AC) applications, is represented by zeolites. Indeed, zeolites are single charge carrier ionic conductors with a temperature-dependent electrical conductivity. In particular, electrical transport in zeolites is due to the monovalent charge-balancing cations, like K^+, capable of hopping between negatively charged sites in the aluminosilicate framework. Owing to the highly non-linear electrical behavior of the traditional electronic NTC materials, the possibility to have alternative types of materials, showing linearity in their electrical behavior, is very desirable. Among different zeolites, natural clinoptilolite has been selected for investigating NTC behavior since it is characterized by high zeolite content, a convenient Si/Al atomic ratio, good mechanical strength due to its compact microstructure, and low toxicity. Clinoptilolite has shown a rapid and quite reversible impedance change under heating, characterized by a linear dependence on temperature. X-ray diffraction (XRD) has been used to identify the natural zeolite, to establish all types of crystalline phases present in the mineral, and to investigate the thermal stability of these phases up to 150 °C. X-ray photoelectron spectroscopy (XPS) analysis was used for the chemical characterization of this natural clinoptilolite sample, providing important information on the cationic content and framework composition. In addition, since electrical transport takes place in the zeolite free-volume, a Brunauer–Emmett–Teller (BET) analysis of the mineral has also been performed.

Keywords: NTC material; zeolite; clinoptilolite; ionic conduction; lamellar texture; sustainability

1. Introduction

Zeolites are lightweight ceramic materials because they have a crystalline lattice, particularly reach in cavities [1–3]. The crystalline lattice of zeolites consists of a three-dimensional aluminosilicate network composed of SiO_4 and AlO_4 tetrahedra connected together by the oxygen atoms [4]. Since negative charges are present in the aluminosilicate framework, extra-framework cations are required for the material electroneutrality condition. Monovalent metal cations are located close to the aluminum atoms in order to balance their negative charges, while bivalent metal cations are positioned halfway between two neighboring negatively charged sites. In particular, the extra-framework ions, typically present in nature-made zeolites, are alkali (K^+, Na^+) and alkaline-earth (Ca^{2+}, Mg^{2+}) metal cations. Since mineral zeolites have mostly aluminous nature, i.e., they are characterized by a low value of the Si/Al ratio, which usually ranges from 4 to 7 [5], a large amount of charge-balancing metal cations is contained. Many natural zeolites also contain iron, which causes

a reddish coloration of the mineral. Iron can be present both in the covalent framework (isomorph substitution of silicon, like in the aluminum case) and/or in the extra-framework, as charge-balancing cations (ferric cations, Fe^{3+}) [6].

Most zeolites, like for example clinoptilolite, are microporous crystalline materials due to the presence of large and small reticular cavities (α and β cages, respectively). These cages are connected to each other to form regular arrays of channels. A schematic representation of the channels present in a clinoptilolite crystal is given in Figure 1. As shown, the silica and alumina tetrahedra, connected together by shared oxygen atoms, form three types of channels that are organized in form of a two-dimensional array. In particular, the A-type (openings: 3.1–7.5 Å) and B-type (openings: 3.6–4.6 Å) channels are parallel to each other and parallel to the c-axis, while the C-type channels (openings: 2.8–4.7 Å), which are parallel to the a-axis, perpendicularly intersect the A and B channels.
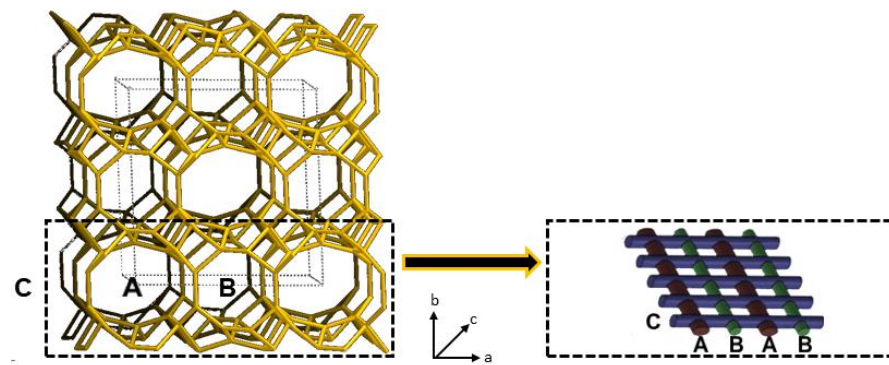
Figure 1. Schematic representation of the channels structure in clinoptilolite crystals.

Extra-framework cations and adsorbed water molecules are located inside these channels, both close to the aluminum atoms. Owing to the strong electrostatic interaction (Coulomb's forces) acting between the extra-framework cations and the negatively charged aluminum atoms, these cations practically do not move under the effect of an electric field at room temperature. Actually, the negative charge is not wholly localized on the aluminum atoms, but it is spread by the mesomeric effect on a 'nucleophilic area', including the aluminum atom and the four neighboring oxygen atoms [7]. Differently, at high temperatures, cations with a low charge density (i.e., K^+ or Na^+) have enough energy for hopping among neighboring empty nucleophilic areas [8]. Empty nucleophilic areas are contained in the zeolite framework because of the bivalent cations, the presence of which leaves a number of unbalanced negative sites in the covalent crystal. Electrical transport in dehydrated zeolites has been investigated by different authors [9,10]. They have formulated an electrical conduction model based on the existence of a 'free ionic conduction zone' in the crystalline lattice [11–13] that consists of free cationic conduction bands located just in the middle of the largest channels (that is, those channels containing super-cages). According to this model, zeolites have negative temperature coefficient behavior; indeed, their resistivity significantly decreases in a linear manner with increasing temperature [14,15]. This fully reversible phenomenon could be advantageously exploited for many technological applications, like for example the fabrication of new types of thermistors for the AC circuits [16], thermal switches/regulators for AC circuits, temperature sensors, and many other types of temperature-related devices [17–22].

Materials adequate for fabricating NTC devices (e.g., a thermal switch capable of turning on reversibly by heating) must have quite a low electrical conductivity at service temperature (e.g., room temperature) and show significant/rapid change in such a value with increases in temperature. This device type could be based on zeolites; however, for showing this special electrical behaviour, the Si/Al atomic ratio is a critical parameter and it needs to have a convenient value because zeolite electrical conductivity strictly depends on it. Among the natural zeolite types, clinoptilolite mineral seems to be the best choice for this application because it has an intermediate value of Si/Al atomic

ratio, which is capable of guaranteeing electrical insolation at room temperature and a significant electrical conductivity increase with heating (good electrical conductor at high temperature). Indeed, the Si/Al atomic ratio typically ranges from 3.5 to 7 in natural zeolites, and it falls close to 5 for clinoptilolite mineral. In addition, this natural zeolite possesses a number of further useful characteristics that are strictly needed for fabricating chip, stable, and robust devices. For example, clinoptilolite is one of the most common types of natural zeolite [23,24], widely available on the market at a very low cost. This material is non-toxic and biocompatible. In addition, differently from other nature-made zeolites, clinoptilolite has good thermal stability (in a wet environment also) and excellent mechanical proprieties for natural ceramics due to the highly compact organization of lamellar crystals in its inner structure [25]. These unique physical/chemical characteristics allow us to use clinoptilolite for fabricating very robust functional devices that are very adequate for industrial exploitations.

Here, the negative temperature coefficient properties of a commercial natural clinoptilolite sample have been investigated. The sample has first been structurally, morphologically, and chemically characterized in order to establish its exact nature. In particular, the type of crystalline phases contained in the mineral and its structural stability up to 150 °C have been investigated by using the X-ray diffraction (XRD) technique. The sample morphology has been visualized by using scanning electron microscopy (SEM). X-ray photoelectron spectroscopy (XPS) has been used to determine the mineral chemical composition and to establish its thermal stability up to 150 °C. In order to achieve optimal results in ultra-high-vacuum (UHV) conditions, XPS tests have been carried out on samples reduced in a powdered form. The specific surface area and pore size of clinoptilolite were also accurately measured by using the Brunauer–Emmett–Teller (BET) analysis, since the electrical transport mechanism takes place only in the material microporosity.

2. Materials and Methods

The clinoptilolite mineral was supplied by T.I.P. (Technische Industrie Produkte, GmbH, Waibstadt, Germany). The natural zeolite stone was mechanically shaped in order to obtain squared monoliths with a thickness of only a few millimeters (see Figure 2a). The squared monoliths were obtained by using a 3-axis computer numerical control (CNC) vertical milling machine (Super proLIGHT 1000, Vertical Machining Center, Intelitek, Derry, NH, USA). The irregularly shaped stone was blocked in a press and successively cut by using a mini metal hacksaw. Then, the sample, glued on a wooden support, was successively clamped in the milling machine vice and machined. The processing cycle included an initial roughing stage to obtain samples with a programmed thickness of ca. 4 mm, which was subsequently reduced to 2.5 mm. In the second stage, square-shaped samples with a size of 10 mm were produced, and an excess of surface material was removed to reach the desired thickness. The electrodes used for electrically characterizing the NTC behavior were fabricated by using a conductive ceramic paste (XeredEx, XD-120, SGS, Beijing, China), and a copper wire with a diameter of 0.6 mm was used for the electrical connections (see Figure 2b).

The nature of the crystalline phases present in the mineral, their percentages, and the zeolitic phase structural stability under heating up to a temperature of 150 °C were investigated by using X-ray diffraction (X'Expert PRO, PANalytical, Oxford, UK). The relative peak intensities were recorded in a 2θ range from 5° to 80°.

The mineral morphological characterization was performed by using scanning electron microscopy (SEM, Quanta 200 FEG microscope, FEI, Hillsboro, OR, USA). In particular, the surface of the mineral was polished, chemically etched, and observed at very high magnification. SEM observation at high magnification is required to visualize the clinoptilolite nanometric texture, which is made of lamellas with an identical thickness of 40 nm. In particular, the sample was first grained and then polished by using a silicon carbide paper with a grit size of 4000 (P4000, Microcut Silicon Carbide grinding paper, USA, Buehler). Owing to the larger number of Si atoms contained in clinoptilolite compared to the Al

atoms (4.6:1 for our zeolite sample), the chemical etching treatment was based on the desilication reaction (i.e., dissolution of the silica framework with formation of soluble sodium silicate). In particular, a sodium hydroxide (NaOH) aqueous solution (2.65 M) was used for the clinoptilolite mineral etching (the sample was treated for 3 h at room temperature). It must be pointed out that an etching treatment based on the dealumination reaction (e.g., treatment by aqueous HCl solution) is not effective since it can only cause the formation of lattice defects.

(**a**) (**b**)
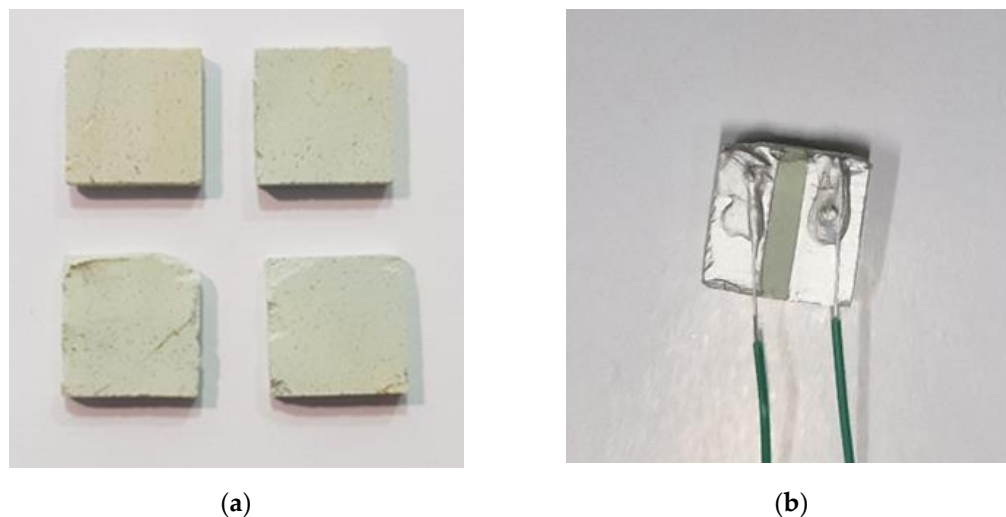
Figure 2. Square-shaped clinoptilolite monoliths (**a**) and electrodes painted on the specimen (**b**).

X-ray photoelectron spectroscopy (XPS) (VG microtech, Uckfield, UK) was used to study the surface chemical composition of mineral samples in the 'as received' and powdered form. XPS measurements were carried out in an ultra-high-vacuum (UHV) chamber equipped with a non-monochromatized X-ray source (Mg K_α photon at 1253.6 eV) and a VSW HA100 hemispherical analyzer (PSP Vacuum Technology Ltd., Macclesfield, UK), with PSP electronic power supply and control, leading to a total energy resolution of 0.86 eV. The binding energy (BE) scale of the XPS spectra was calibrated using the Au 4f peak at 84.0 eV as a reference. Quantitative analysis was performed on core levels by using Voigt line-shape deconvolution after background subtraction of a Shirley function (the atomic percentages were determined with an error of $\pm 0.25\%$). Zeolite in powdered form was the preferential choice for surface analysis due to its low outgas in UHV; however, several annealing temperatures of up to 150 °C were necessary on the natural bulk stone, so as to check its thermal stability in order to obtain the same results as in the powder case.

Nitrogen adsorption analysis was performed on clinoptilolite by means of a 3Flex adsorption analyzer (Micromeritics, Norcross, GA, USA). N_2 adsorption/desorption isotherms were recorded at 77 K and SSA was determined by nitrogen from the linear part of the Brunauner–Emmett–Teller (BET) equation. The pore volume of clinoptilolite was calculated from the N_2 adsorption isotherm at a 0.85 p/p_0. The nonlocal density functional theory (NLDFT) was applied to the N_2 adsorption isotherm to evaluate the micro/mesopore size distributions. Before the analysis, the sample was degassed at 120 °C under vacuum ($p < 10^{-7}$ mbar). The adsorption measurements were performed by using high-purity gases (>99.999%).

Electrical transport in high impedance ionic conductors (i.e., MΩ magnitude order) can be easily investigated. Indeed, a sinusoidal voltage, produced by a function generator, can be applied to this high-impedance conductor without the risk of overloading the equipment, since the resulting electrical current intensity has quite a low value (μA-nA magnitude order) for the high impedance value. Owing to the very high signal stability, direct digital synthesis (DDS) function generators represent the most suitable sigmoidal voltage sources. The intensity of this micro/nano-currents can be measured as effective

values (root-mean-square, RMQ) by using the large-bandwidth AC microammeter of a digital multimeter (DMM). The DMM bandwidth should be high enough to allow for the measurement of voltage signals with a frequency higher than 1 kHz, which is required to avoid electrode polarization phenomena. Such a device may also include a datalogger system for recording the current intensity measurements made during that time.

Zeolites are ionic conductors with a single charge carrier, characterized by a very high impedance value; this physical characteristic allows us to study these ceramic conductors by using such a simple approach. Two electrodes were placed on the surface of the square-shaped clinoptilolite monolith in order to test the material electric behavior under fast uncontrolled heating, which was achieved by using a high-power light bulb as the heat source. The electric current intensity was measured by the true-RMS DMM, which was placed in series with the sinusoidal signal generator (see Figure 3). The square-shaped clinoptilolite sample was connected to an AC voltage source (sinusoidal voltage signal of 20 V_{pp}, 5 kHz) and the current intensity flowing in it was measured by setting the wide-band true-RMS DMM as the AC microammeter. Before the electrical tests, the samples were stored for 24 h in a cabinet containing activated silica gel. This mild dehydration treatment of the clinoptilolite device is required to avoid an excessive water molecule release phenomenon during the electrical measurement. Electrical signals were measured and recorded during the time by using the devoted DMM datalogger software.
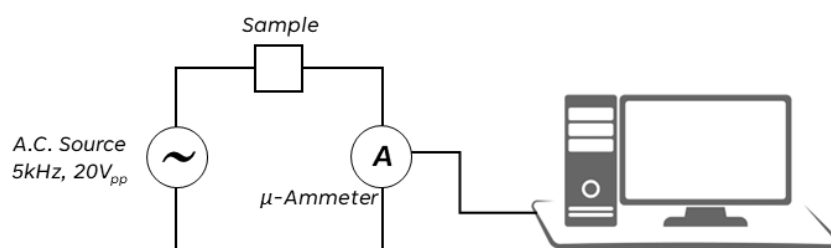

Figure 3. Schematic representation of the electric circuit used for tests.

In particular, a direct digital synthesis (DDS) function generator (Gratten, ATF20B+, Atten.Eu, Helmond, The Netherlands) was used as the voltage source, and a true-RMS, 10 kHz bandwidth, DMM (UT61E, Uni-Trend Technology, Dongguan, China) was used as the AC microammeter. The effective current intensity value (I_{eff}) was recorded on a PC equipped with a devoted datalogging software (UT61E-Software v.01, Uni-Trend Technology, Dongguan, China). Fast specimen heating was achieved by placing its bottom-side surface in contact with the glass bulb surface of a high-power halogen lamp (NT U H4, 12 V, 60/55 W, P43T), powered up by a DC power supply (LABPS 3005D, 30 V/5 A, Velleman, Gavere, Belgium). In order to facilitate heat transfer from the heat source (i.e., the bulb) to the sample, the clinoptilolite specimen had a reduced thickness (2.5 mm) and, in addition, a silver conductive paste was placed between sample and light bulb. Successively, the following electrical test was performed: the sample was heated slowly and in a calibrated manner by using an aluminum block containing a ceramic heating cartridge. A layer of Kapton/cotton wadding thermally insulated the sample (for this purpose, the heating block set of a 3D printer was used). A digital datalogger thermometer (UT-325, Uni-Trend Technology, Dongguan, China) was used to measure and record sample temperature over the time.

3. Results

In order to establish the exact nature of the crystalline phases contained in the commercial zeolite sample, the mineral was first characterized by using X-ray diffraction (XRD). Since zeolites and other minerals have a crystalline nature, XRD represents a very convenient approach to identifying all the solid phases present in the sample. As visible in Figure 4, the XRD patterns of the mineral showed the diffraction peaks of clinoptilolite and cristobalite (quartz) phases. In particular, the most intensive characteristic signals of

clinoptilolite can be detected at 9.8446°, 22.4026°, 30.0076°, and 31.9576° [26]. According to this XRD analysis, the clinoptilolite phase was ca. 65% by weight and the cristobalite phase was ca. 35% by weight.
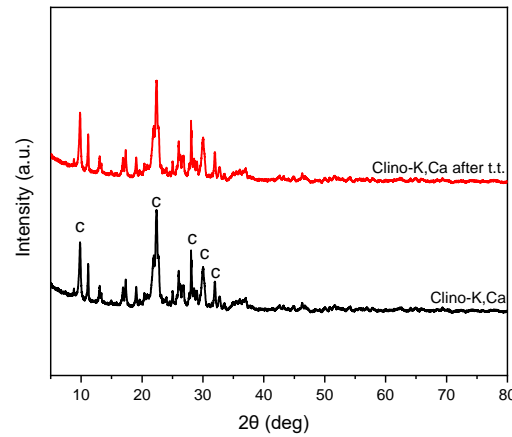
Figure 4. XRD patterns of clinoptilolite sample before (black line) and after (red line) a thermal treatment (t.t.) of 5 h at 150 °C.

XRD was also used to establish the thermal stability of the clinoptilolite phase in the temperature range involved in the electrical tests. As clearly visible in Figure 4, the diffraction pattern of the clinoptilolite sample after a thermal annealing treatment at 150 °C appeared practically unmodified, thus indicating the high structural stability of the mineral at this temperature range.

The scanning electron microscopy (SEM) micrographs of the etched mineral sample surface (see Figure 5a,b) clearly show the typical clinoptilolite microstructure, which is made of tendentially iso-oriented stacks of lamellar crystals. All clinoptilolite lamellas have the same thickness (40 nm), while the other two sizes are of a few hundred microns. Such lamellar morphology is a characteristic of clinoptilolite crystals [10,27]; however, a similar microstructure can be found also in many other nature-made materials [28]. The good mechanical performance of this zeolite type can only be ascribed to this special morphology. Owing to the high clinoptilolite content, the electrically conductive zeolite lamellar crystals are interconnected and form a continuous percolation network with paths crossing the full solid structure.

(**a**)   (**b**)
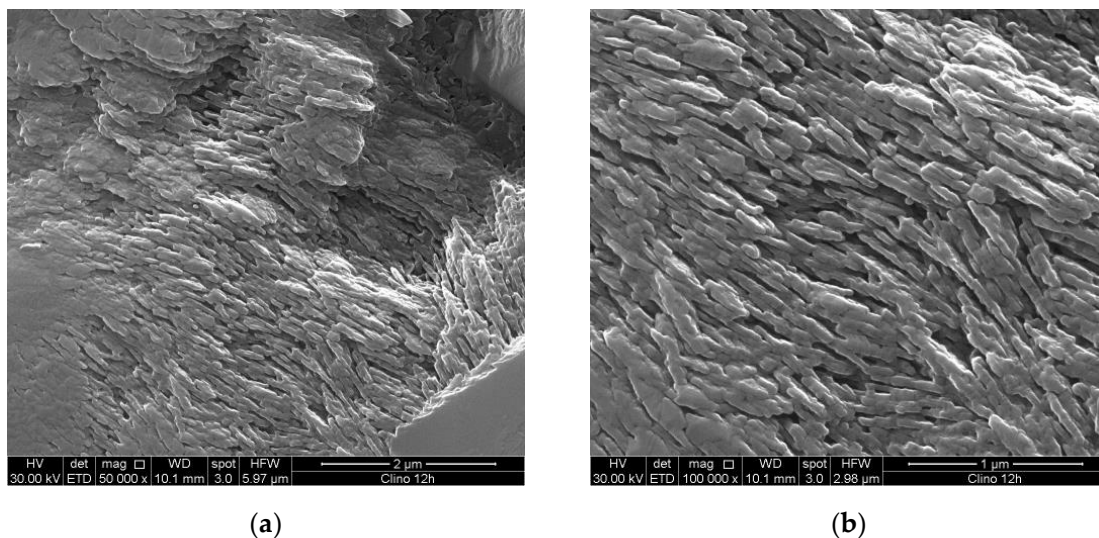
Figure 5. SEM micrographs of the etched clinoptilolite mineral surface at different magnifications (**a**,**b**).

The chemical composition obtained by X-ray photoelectron spectroscopy (XPS) analysis (Figure 6a) revealed the presence of Si (Si2p), Al (Al2p), and O(O1s) as framework elements, and Ca (Ca2p) and K (K2p) as extra-framework elements. A small amount of Fe (Fe2p) was also identified (Figure 6b); it shows a broad and complex core level line-shape, suggesting the presence of iron in different chemical configurations, likely Fe both in the framework and extra-framework positions.
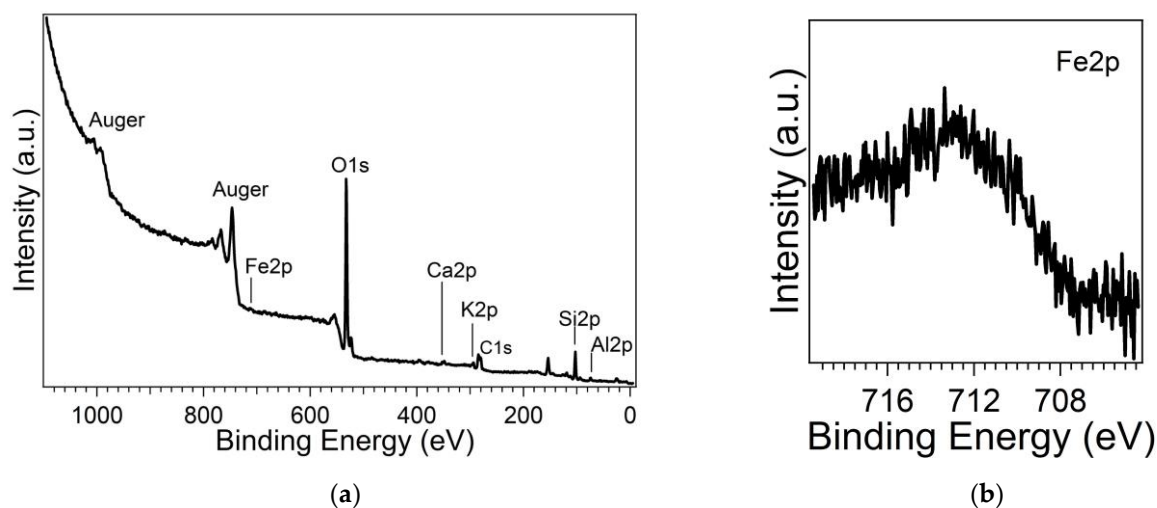
Figure 6. XPS long-range (**a**) and Fe2p (**b**) (pass energy 50 eV) spectra of natural clinoptilolite powder.

A BE shift in all core levels due to charging phenomena of about 5.6 eV was observed (taking into account the energy reference from adventitious carbon at 285 eV). Al2p and Si2p BE positions are 74.5 eV and 102.9 eV (main), respectively, which is in agreement with the literature [29,30]. Table 1 reports the chemical composition in the surface as atomic percentages. Deviations from the bulk composition of natural clinoptilolite are expected due to the high surface sensitivity of this technique, the sampling depth of which is within few nanometers from the surface [31]. Since it was found that K and Ca elements have comparable concentrations in the mineral sample, zeolite can be classified as clinoptilolite-K, Ca.

Table 1. Surface atomic percentages of Al, Si, O, Ca, K, and Fe as calculated from XPS on clinoptilolite powder.

XPS Signals	Al2p	Si2p	O1s	Ca2p	K2p	Fe2p	Si/Al
at. %	7.22	33.22	56.42	1.30	1.71	0.13	4.60

The chemical composition as obtained by XPS vs. sample temperature is shown in Figure 7. As visible, the chemical composition is mostly unchanged with the increase in temperature up to 150 °C. Therefore, according to the XRD and XPS results, this natural ceramic sample can be considered to have high thermal stability in the temperature range adopted for the electrical characterization.

The nitrogen adsorption/desorption analysis (see Figure 8) showed that the clinoptilolite powder has a BET specific surface area of 25 ± 0.1 m^2/g and a total pore volume of 0.032 cm^3/g. NLDFT pore distribution analysis showed the presence of both microporous and mesoporous fractions in the specimen. In particular, a significant portion of porosity (about 16%) is narrowly centered at 1.4 nm, which is compatible with zeolite crystalline microporosity; the remaining (meso)porosity extends mainly from 3 nm to 20 nm and is ascribable to the interlamellar space. These results are in line with those reported in the literature for several specimens of natural clinoptilolite of different origins that have not undergone acid or high-temperature calcination treatments [32–35].
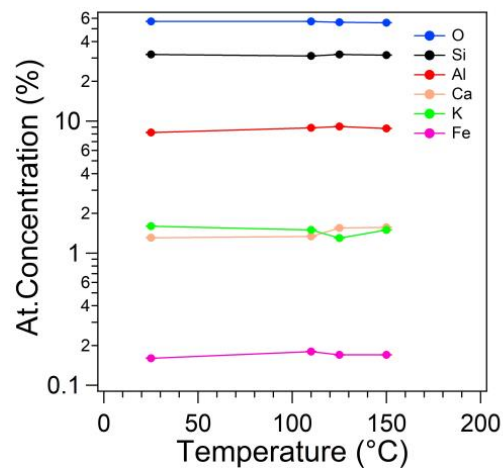
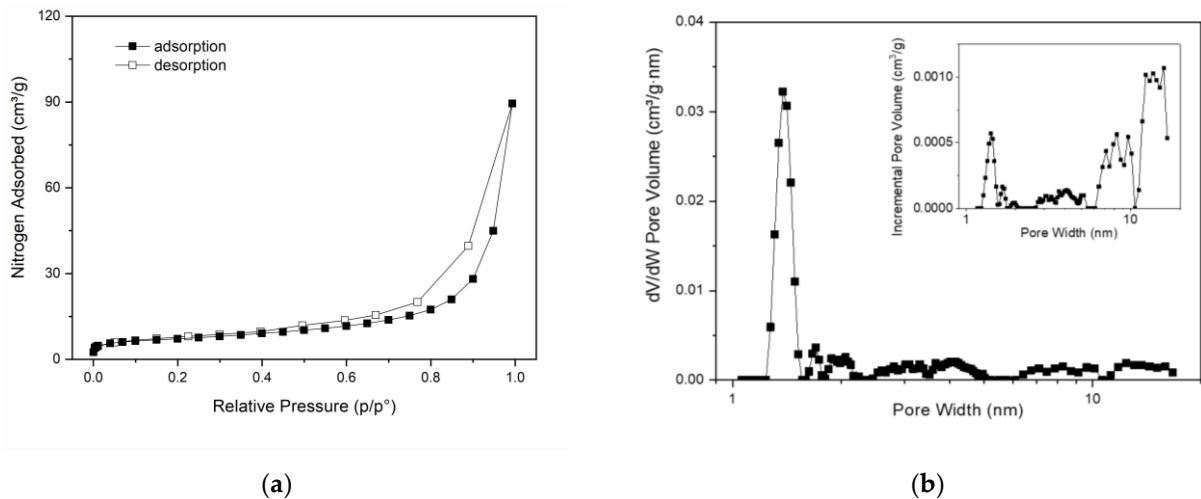**Figure 7.** Surface atomic percentages of clinoptilolite-K, Ca, after thermal treatments in UHV.


(**a**) (**b**)

Figure 8. Nitrogen adsorption/desorption isotherm (**a**) and NLDFT pore size distribution (**b**) of clinoptilolite.

The effect of a rapid increase in temperature on the mobility of the extra-framework cations (actually, K^+ is the only charge carrier present in the system) was investigated by monitoring under a constant sinusoidal voltage value and the variation in the effective current intensity flowing in the specimen during the heating process.

As visible in Figure 9a, the application of a thermal pulse to the clinoptilolite monolith promptly generated an electrical micro-current in the ceramic sample. This micro-current grew very quickly with the increase in time after turning on the lamp. During the successive cooling step in air (i.e., turning off the incandescent lamp), the micro-current intensity readily decreased until it reached its starting value, negligibly. The resulting current intensity peak had quite an asymmetric profile because the process of sample cooling in air was slower than the previous heating process. In particular, the heating step followed a linear behavior (see inset in Figure 9b) with a slope of (13.8 ± 0.1) μA/s, while the cooling step followed a hyperbole law. Figure 9b shows the sample behavior under repeated heating/cooling cycles; as visible, four repeated cycles were unable to modify the electric behavior of these NTC materials. The higher value of current intensity that is usually recorded during the first heating step (see Figure 9b) probably represents a hysteresis in the electrical behavior of the dehydrated clinoptilolite sample. Indeed, before electrical characterization, the ceramic samples were only mildly dehydrated by using well-activated silica gel (activation conditions: 5 h at 150 °C under vacuum) and some water molecules (i.e., loosely-bound water [36]) were still present inside the clinoptilolite

channels. According to the Vučelić model of the 'free ionic conduction zone' [12], these residual water molecules which are adsorbed on the surface of channel walls promote the electrical transport in the material. Differently, water molecules are mostly removed from the sample during the first heating step that takes place at quite high temperatures; therefore, the sample's electrical conductivity results reduce in all the successive heating cycles of the electrical test, as is shown in Figure 9b.

(**a**) (**b**)
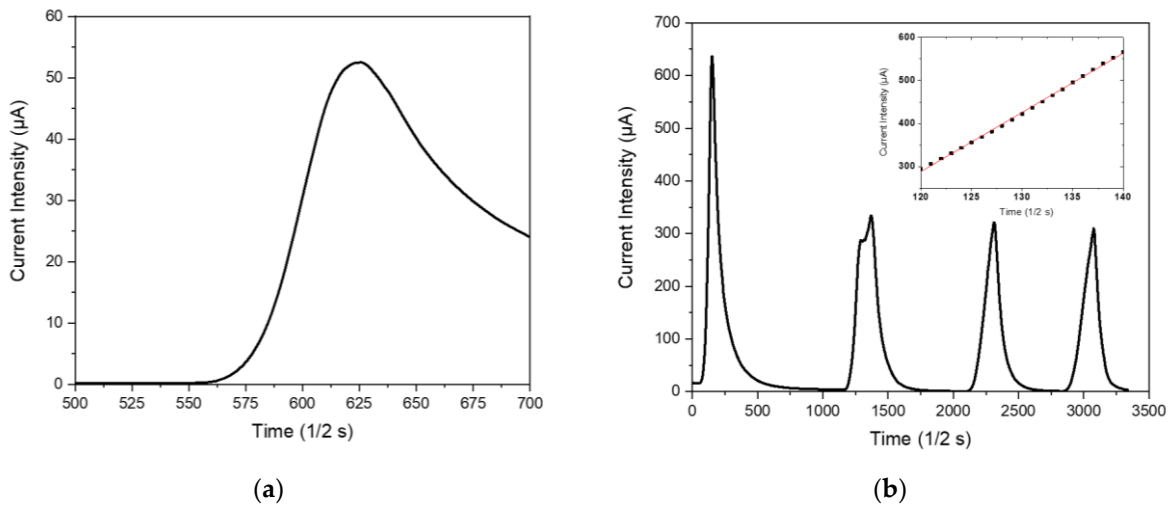
Figure 9. Temporal evolution of effective current intensity with the turning on/off of the heat source (**a**) and NTC material behavior under repeated thermal pulses (**b**). Linearity of the temporal current intensity behavior is shown in the inset.

Since during the electrical tests the sinusoidal generator provides a constant voltage value of 20 V$_{pp}$, the sample impedance (Z) can be calculated by using the measured current intensity values. The temporal evolution of the calculated Z value is shown in Figure 10a. As visible, the heating process produces a significant decrease in Z that can be conveniently represented by using a logarithmic scale; indeed, the Z value changes in 2–3 magnitude orders during the heating/cooling process. In particular, like for the current intensity, Z varies quite linearly during the heating stage, while it decreases non-linearly during the sample cooling back to room temperature. According to the slope of the linear temporal behavior of Z, this quantity changes very quickly with the increase in time, and the switching process occurs mostly reversible. A hysteresis in the Z value is associated with only the first heating/cooling cycle of the electrical test, as shown in Figure 10b.

(**a**) (**b**)
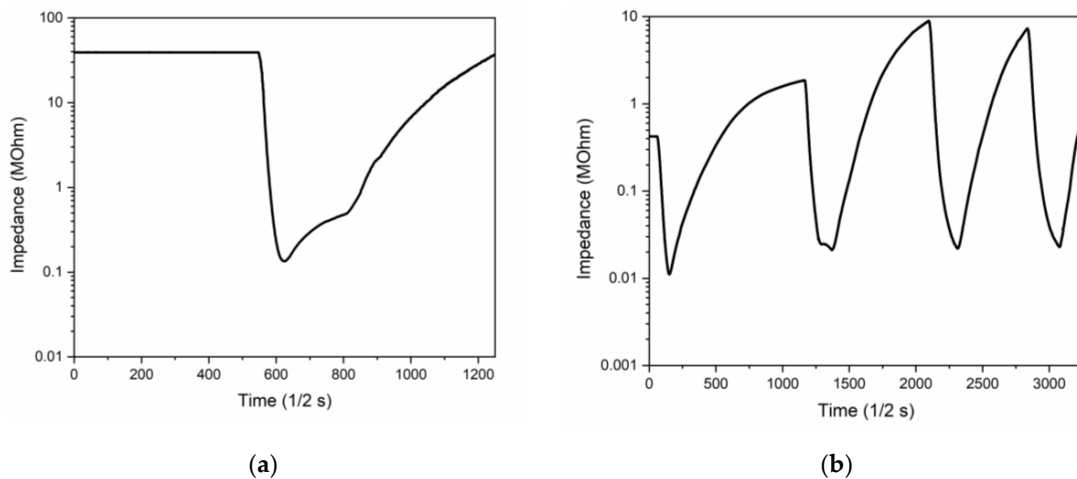
Figure 10. Temporal evolution of Z with the turning on/off of the heat source, (**a**) and NTC material impedance behavior under repeated thermal pulses (**b**).

Heating tests at known temperature values were also performed by using a similar approach based on time-resolved effective current intensity measurements (see Figure 11). In this case, both the current intensity and calculated impedance curves are given as a function of the temperature, which was also measured during the time. As visible in Figure 11, a slow/controlled heating process was capable of giving quite a asymmetric I_{eff}-T peak, just like in the case of a thermal pulse.

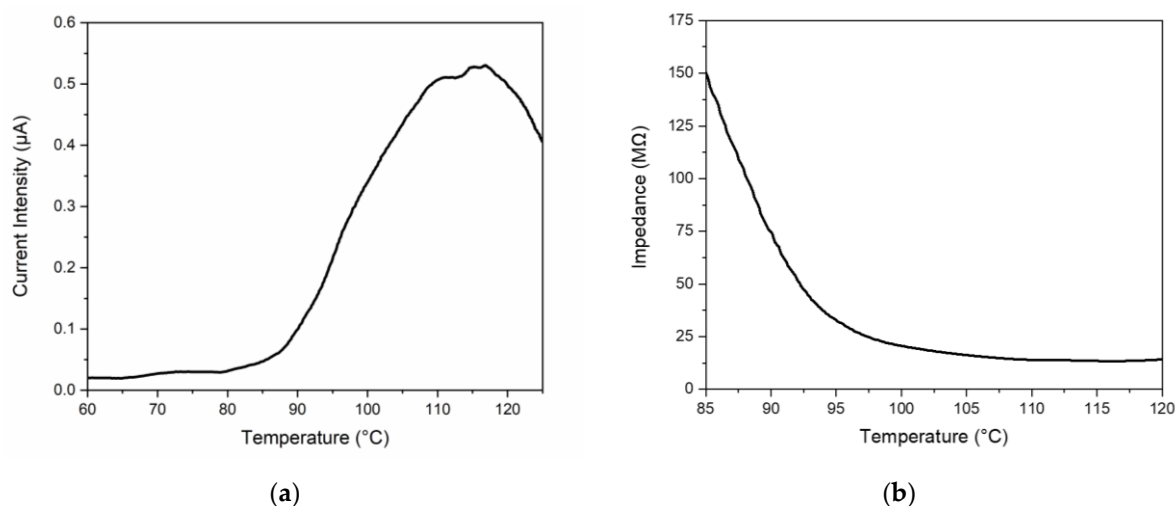(**a**)   (**b**)

Figure 11. I_{eff}-T curve (**a**) and related impedance curve (**b**).

4. Discussion

Zeolites are low-density crystalline aluminosilicates with unique physical properties that result from their unusual chemical structure. This special class of compounds has a covalent crystalline structure with extra-framework positive charges (namely charge balancing cations) placed on the walls of the crystal cavities, close to the aluminum negative charges. Vučelić defined this extraordinary crystalline structure as a 'reverse' metallic lattice [11]. According to the electrical conduction model proposed by Vučelić in 1977 [12,13], only those extra-framework charges capable of moving in the 'free ionic conduction zones', i.e., the free cationic conduction bands located exactly in the middle of crystal channels, can promote electrical transport trough the ceramic material. Indeed, ions at the centers of cavities are effective carriers of current since they move through the zeolite crystal with only minimal activation energy. This interesting model proposed by Vučelić constitutes an analogous depiction of the behavior of electrons in a fixed cationic electromagnetic field and their electrical conduction mechanism. Therefore, Vučelić has conformed zeolites to the commonly adopted representation of electrical transport in metallic crystal structures.

The electrical properties of zeolites mainly depend on the contained monovalent metal ions because they are less strongly held by the negatively charged lattice and can easily migrate between two neighboring negative sites through the free ionic conduction zones. In more detail, the electrical conductivity of clinoptilolite, $\sigma(T)$, depends only on the following three factors: (i) charge of the electrical carriers: Ze^-, where e^- is the elementary charge ($e^- = 1.602 \times 10^{-19}$ C); (ii) concentration of the electrical carriers: $[Me^{Z+}]$; and (iii) mobility of the electrical carriers: μ, according to the following physical law: $\sigma(T) = \Sigma_i[Z_i \cdot e^- \cdot [Me^{z+}]_i \cdot \mu_i]$, where the sum is formally extended to all extra-framework cations present in the substance. However, since the tested sample is clinoptilolite-K, Ca, potassium ions located in the super-cages are almost exclusively involved in the migration under the applied sinusoidal field (5 kHz, 20 V_{pp}). Indeed, the contribution of Ca^{2+} cations is negligible because they have an electrical charge larger than K^+ and are present in the clinoptilolite sample at a lower concentration. Iron does not participate in the electrical transport mechanism because it is mostly located in the framework (isomorphous substitution), just like in the case of aluminum atoms, while its ionic form (Fe^{3+}) has a very

large electrical charge and stably adheres to the crystal framework. Finally, it is possible to approximately write:

$$\sigma(T) = e^- \cdot [K^+]^* \cdot \mu_{K+}$$

where $[K^+]^*$ is the molar concentration of the excited K^+ cations present in the system at T temperature. Each K^+ ion is located in a potential well (the 'nucleophilic area'), the walls of which are represented by the four negatively charged oxygen atoms located close to the aluminum atom [10]. The concentration of excited K^+ present at a zeolite cage/channel center is a temperature-dependent quantity; indeed, $[K^+]^*$ increases with increasing temperature, thus determining an increase in the zeolite electrical conductivity.

Clinoptilolite is a unique ionic conductor, and its physical, chemical, mechanical, and electrical properties have been deeply investigated. Since different useful characteristics are combined together in clinoptilolite and other zeolites, these multifunctional inorganic materials have great potentialities for industrial applications. For example, mechanically robust and thermally stable impedimetric sensors based on zeolite have been described in the literature [37–42]. However, such ionic conductors could also have further technological potentialities in other important areas of electronics (e.g., radiofrequency filters, dielectrics for electrolytic capacitors, electrolytic pastes, etc.). Although clinoptilolite has many useful electrical properties, the literature articles describing the fabrication/characterization of electrical devices based on clinoptilolite are still very limited. The aim of this manuscript is to introduce the possibility of developing a new concept of thermistor and other NTC devices for AC applications by exploiting the strict temperature dependence of clinoptilolite ionic conductivity. For example, NTC materials are widely used in the control electronics industry for the protection of electronic circuits.

The reason natural clinoptilolite has been selected among the different zeolites is mainly related to the following: (i) the very good mechanical properties, (ii) the high thermal resistance of the porous crystalline structure, and (iii) the significant electrical conductivity changes rising temperature. Such a unique property combination makes zeolite an interesting technological solution; indeed, other ionic conductors do not have high thermal stability or do not have the linear dependence of electrical conductivity on temperature as observed for clinoptilolite. In addition, natural clinoptilolite is a widely available mineral with a good zeolitic content and a very low cost. Depending on the extraction mine, this mineral can have slightly different chemical compositions (i.e., Si/Al atomic ratio and type/percentage of extra-framework cations); however, it can always be used for electrical applications even on a large-scale (e.g., grounding enhancement materials [43] and gas discharge electronic devices [44,45]). The NTC behavior of clinoptilolite can be advantageously exploited to develop new types of thermistors that are adequate for application in AC circuits. Indeed, zeolites are ionic conductors with single charge carriers and they therefore require AC conditions for electrical transport. This type of device is different from those already available, which are based on ceramic semiconductors, as their use is limited to DC circuits.

Here, the thermistors were fabricated by using the unmodified geomorphic material, which was just shaped in form of squared plates. However, such zeolite-based devices can undergo a number of technical improvements as in the fabrication of electrodes with high thermal stability: device encapsulation or surface treatment to prevent moisture adsorption in the microporous structure; electrical conductivity control (increase/decrease) by changing the type of charge carrier; development of devices based on zeolite coatings on plastic/ceramic substrates, etc. Such points will be investigated in our future research work.

5. Conclusions

Clinoptilolite is an electrically conductive material (single charge carrier ionic conductor), and its impedance value has shown a strict dependence on temperature. In particular, surface impedance of clinoptilolite changes readily, substantially, linearly, and reversibly with heating in the temperature range of 25–120 °C and above. This electrical performance allows us to suggest the use of NTC devices based on this zeolite type for AC electronic

circuits applications as an alternative to traditional semiconductor-based devices. According to the morphological investigations made by using SEM, the sample consists of 40 nm thick single lamellar crystals that are closely compacted together. Such a microstructure allows us to achieve good mechanical performance and extended percolative paths in the sample, which are essential for a uniform electrical conductivity. Since the electrical transport phenomenon takes place in the clinoptilolite channels, the specific surface area and porosity were determined by using BET analysis. In particular, it was found that the raw material is characterized by a surface area of $25 \pm 0.1 \text{ m}^2/\text{g}$ and pores with an average size ranging from 1.4 to 20 nm. The sample crystalline composition was determined by using XRD, revealing the clinoptilolite phase as the main mineral component (65% by weight); in addition, its thermal stability up to 150 °C was verified too. The chemical analysis of sample surface was performed by using XPS. In particular, XPS analysis provided an atomic Si/Al ratio of 4.6, and K^+ and Ca^{2+} were found to be extra-framework cations present on the sample surface. Therefore, the monovalent K^+ cation is the charge carrier responsible for the system's AC electrical transport. The XPS surface analysis has also provided information on the nature of the contained iron, which is present both in the mineral framework and extra-framework regions.

References

1. Misaelides, P. Application of natural zeolites in environmental remediation: A short review. *Microporous Mesoporous Mater.* **2011**, *144*, 15–18. [CrossRef]
2. Jha, B.; Singh, D.N. Basics of Zeolites. In *Fly Ash Zeolite: Innovations, Applications, and Directions*; Part of the Book Series: Advanced Structured Materials; Springer: Singapore, 2016; Volume 78, pp. 5–13. [CrossRef]
3. Auerbach, S.M.; Carrado, K.A.; Dutta, P.K. (Eds.) *Handbook of Zeolite Science and Technology*, 1st ed.; CRC Press: Boca Raton, FL, USA, 2003; p. 1204. [CrossRef]
4. Koohsaryan, E.; Anbia, M. Nanosized and Hierarchical Zeolites: A Short Review. *Chin. J. Catal.* **2016**, *4*, 447–467. [CrossRef]
5. Wang, C.; Leng, S.; Guo, H.; Yu, J.; Li, W.; Cao, L.; Huang, J. Quantitative Arrangement of Si/Al Ratio of Natural Zeolite Using Acid Treatment. *Appl. Surf. Sci.* **2019**, *498*, 143874. [CrossRef]
6. Aiello, R.; Nagy, J.B.; Giordano, G.; Katovic, A.; Testa, F. Isomorphous Substitution in Zeolites. *Comptes Rendus Chim.* **2005**, *8*, 321–329. [CrossRef]
7. Uzunova, E.L.; Mikosch, H. Cation Site Preference in Zeolite Clinoptilolite: A Density Functional Study. *Microporous Mesoporous Mater.* **2013**, *177*, 113–119. [CrossRef]
8. Ohgushi, T.; Ishimaru, K.; Adachi, Y. Movements and Hydration of Potassium Ion in K-A Zeolite. *J. Phys. Chem. C* **2009**, *113*, 2468–2474. [CrossRef]
9. Schäf, O.; Ghobarkar, H.; Adolf, F.; Knauth, P. Influence of Ions and Molecules on Single Crystal Zeolite Conductivity under in Situ Conditions. *Solid State Ion.* **2001**, *143*, 433–444. [CrossRef]
10. Kelemen, G.; Schön, G. Ionic Conductivity in Dehydrated Zeolites. *J. Mater. Sci.* **1992**, *27*, 6036–6040. [CrossRef]

11. Vučelić, D.; Juranić, N.; Macura, S.; Šušić, M. Electrical conductivity of dehydrated zeolites. *J. Inorg. Nucl. Chem.* **1975**, *37*, 1277–1281. [CrossRef]
12. Vučelić, D. Ionic Conduction Bands at Zeolite Interfaces. *J. Chem. Phys.* **1977**, *66*, 43–47. [CrossRef]
13. Vučelić, D.; Juranić, N. The effect of sorption on the ionic conductivity of zeolites. *J. Inorg. Nucl. Chem.* **1976**, *38*, 2091–2095. [CrossRef]
14. Jack, K.E.; Etu, I.A.; Nwangwu, E.O.; Osuagwu, E.U. A simple thermistor design for industrial temperature measurement. *IOSR J. Electr. Electron. Eng.* **2016**, *11*, 57–66. [CrossRef]
15. Becker, J.A.; Green, C.B.; Pearson, G.L. Properties and Uses of Thermistors-Thermally Sensitive Resistors. *Bell Syst. Tech. J.* **1947**, *26*, 170–212. [CrossRef]
16. Kamat, R.K.; Naik, G.M. Thermistors—In Search of New Applications, Manufacturers Cultivate Advanced NTC Techniques. *Sens. Rev.* **2002**, *22*, 334–340. [CrossRef]
17. Wang, T.; Chu, Y.; Li, X.; Liu, Y.; Luo, H.; Zhou, D.; Deng, F.; Song, X.; Lu, G.; Yu, J. Zeolites as a Class of Semiconductors for High-Performance Electrically Transduced Sensing. *J. Am. Chem. Soc.* **2023**, *145*, 5342–5352. [CrossRef] [PubMed]
18. Kakhki, R.M.; Zirjanizadeh, S.; Mohammadpoor, M. A review of clinoptilolite, its photocatalytic, chemical activity, structure and properties: In time of artificial intelligence. *J. Mater. Sci.* **2023**, *58*, 10555–10575. [CrossRef]
19. Simon, U.; Franke, M.E. *Ionic Conductivity of Zeolites: From Fundamentals to Applications, Host-Guest-Systems Based on Nanonporous Crystals*; Laeri, F., Schüth, F., Simon, U., Wark, M., Eds.; Wiley-VCH Verlag GmbH & Co. KGaA: Weinheim, Germany, 2003; pp. 364–378. [CrossRef]
20. Qiu, P.; Huang, Y.; A Secco, R.; Balog, P.S. Effect of multi-stage dehydration on electrical conductivity of zeolite A. *Solid State Ionics* **1999**, *118*, 281–285. [CrossRef]
21. Freeman, D.C.; Stamires, D.N. Electrical conductivity of synthetic zeolites. *J. Chem. Phys.* **1961**, *35*, 799–806. [CrossRef]
22. Ghobarkar, H.; Schäf, O.; Guth, U. Zeolites—From kitchen to space. *Prog. Solid State Chem.* **1999**, *27*, 29–73. [CrossRef]
23. Hernández, M.; Hernández, G.I.; Portillo, R.I.; Velasco, M.d.L.; Santamaría-Juárez, J.D.; Rubio, E.; Petranovskii, V. Influence of Chemical Pretreatment on the Adsorption of N_2 and O_2 in Ca-Clinoptilolite. *Separations* **2023**, *10*, 130. [CrossRef]
24. Mastinu, A.; Kumar, A.; Maccarinelli, G.; Bonini, S.A.; Premoli, M.; Aria, F.; Gianoncelli, A.; Memo, M. Zeolite Clinoptilolite: Therapeutic Virtues of an Ancient Mineral. *Molecules* **2019**, *24*, 1517. [CrossRef]
25. Kowalczyk, P.; Sprynskyy, M.; Terzyk, A.P.; Lebedynets, M.; Namieśnik, J.; Buszewski, B. Porous Structure of Natural and Modified Clinoptilolites. *J. Colloid Interface Sci.* **2006**, *297*, 77–85. [CrossRef]
26. Lin, H.; Liu, Q.; Dong, Y.; Chen, Y.; Huo, H.; Liu, S. Study on Channel Features and Mechanism of Clinoptilolite Modified by LaCl3. *J. Mater. Sci. Res.* **2013**, *2*, 37. Available online: https://pdfs.semanticscholar.org/e6d9/b21c22f70922b3b4ef7eda46c9897c858009.pdf (accessed on 1 March 2024). [CrossRef]
27. Schiavo, L.; Cammarano, A.; Carotenuto, G.; Longo, A.; Palomba, M.; Nicolais, L. An overview of the advanced nanomaterials science. *Inorganica Chim. Acta* **2024**, *559*, 121802. [CrossRef]
28. Grüenert, W.; Muhler, M.; Schröder, K.P.; Sauer, J.; Schlögl, R. Anisotropic mechanical behaviors and their structural dependences of crossed-lamellar structure in a bivalve shell. *Mater. Sci. Eng.* **2016**, *59*, 828–837. [CrossRef]
29. Gruenert, W.; Muhler, M.; Schroeder, K.-P.; Sauer, J.; Schloegl, R. Investigations of Zeolites by Photoelectron and Ion Scattering Spectroscopy. 2. A New Interpretation of XPS Binding Energy Shifts in Zeolites. *J. Phys. Chem.* **1994**, *98*, 10920–10929. [CrossRef]
30. Schiavo, L.; Boccia, V.; Aversa, L.; Verucchi, R.; Carotenuto, G.; Valente, T. Natural Clinoptilolite Nanoplatelets Production by a Friction-Based Technology. *Mater. Proc.* **2023**, *14*, 11. [CrossRef]
31. Avval, T.G.; Carver, V.; Chapman, S.C.; Bahr, S.; Dietrich, P.; Meyer, M.; Thißen, A.; Linford, M.R. Clinoptilolite, a type of zeolite, by near ambient pressure-XPS. *Surf. Sci. Spectra* **2020**, *27*, 014007. [CrossRef]
32. Garcia-Basabe, Y.; Rodriguez-Iznaga, I.; de Menorval, L.-C.; Llewellyn, P.; Maurin, G.; Lewis, D.W.; Binions, R.; Autie, M.; Ruiz-Salvador, A.R. Step-wise dealumination of natural clinoptilolite: Structural and physicochemical characterization. *Microporous Mesoporous Mater.* **2010**, *135*, 187–196. [CrossRef]
33. Favvas, E.P.; Tsanaktsidis, C.G.; Sapalidis, A.A.; Tzilantonis, G.T.; Papageorgiou, S.K.; Mitropoulos, A.C. Clinoptilolite, a natural zeolite material: Structural characterization and performance evaluation on its dehydration properties of hydrocarbon-based fuels. *Microporous Mesoporous Mater.* **2016**, *225*, 385–391. [CrossRef]
34. Korkuna, O.; Leboda, R.; Skubiszewska-Zięba, J.; Vrublevs'ka, T.; Gun'ko, V.M.; Ryczkowski, J. Structural and physicochemical properties of natural zeolites: Clinoptilolite and mordenite. *Microporous Mesoporous Mater.* **2006**, *87*, 243–254. [CrossRef]
35. Wahono, S.K.; Prasetyo, D.J.; Jatmiko, T.H.; Suwanto, A.; Pratiwi, D.; Hernawan; Vasilev, K. Transformation of Mordenite-Clinoptilolite Natural Zeolite at Different Calcination Temperatures. In Proceedings of the IOP Conference Series: Earth and Environmental Science, Tangerang, Indonesia, 1–2 November 2018; Volume 251, p. 012009. [CrossRef]
36. Knowlton, G.D.; White, T.R.; McKague, H.L. Thermal Study of Types of Water Associated with Clinoptilolite. *Clays Clay Miner.* **1981**, *29*, 403–411. [CrossRef]
37. Carotenuto, G. Sensing Device for Breath Rate Monitoring Fabricated by using Geomorphic Natural Clinoptilolite. *J. Adv. Biotechnol. Bioeng.* **2020**, *8*, 3–10. [CrossRef]
38. Carotenuto, G.; Camerlingo, C. Zeolite-Based Fast-Responding Sensors for Respiratory Rate Monitoring. *Proceedings* **2019**, *42*, 9. [CrossRef]

39. Schäf, O.; Wernert, V.; Ghobarkar, H.; Knauth, P. Microporous Stilbite single crystals for alcohol sensing. *J. Electroceramics* **2006**, *16*, 93–98. [CrossRef]
40. Urbiztondo, M.; Irusta, S.; Mallada, R.; Pina, M.P.; Santamaría, J. Evaluation of optical and dielectrical properties of the zeolites. *Desalination* **2006**, *200*, 601–603. [CrossRef]
41. Kurzweil, P.; Maunz, W.; Plog, C. Impedance of zeolite-based gas sensors. *Sens. Actuators B Chem.* **1995**, *25*, 653–656. [CrossRef]
42. Reiß, S.; Hagen, G.; Moos, R. Zeolite-based impedimetric gas sensor device in low-cost technology for hydrocarbon gas detection. *Sensors* **2008**, *8*, 7904–7916. [CrossRef]
43. Sitorus, H.B.H.; Permata, D.; Wicaksono, A. A study on the use of powder zeolite as backfill material for single rod grounding system. *IOP Conf. Ser. Mater. Sci. Eng.* **2021**, *1125*, 012075. [CrossRef]
44. Orbukh, V.I.; Lebedeva, N.N.; Ozturk, S.; Ugur, S.; Salamov, B.G. Gas discharge electronic device based on the porous zeolite. *Optoelectron. Adv. Mat.* **2012**, *6*, 947–952.
45. Koseoglu, K.; Ozer, M.; Salamov, B.G. Electrical properties of microdischarge in porous zeolites. *Plasma Process. Polym.* **2014**, *11*, 1018–1027. [CrossRef]